

INTERNAL-NODE WAVEFORM PROBING OF MMIC POWER AMPLIFIERS

C. J. Wei, Y. A. Tkachenko and J. C. M. Hwang
 Lehigh University, 19 Memorial Dr W, Bethlehem PA 18015
 K. E. Smith
 Cascade Microtech, Inc.
 14255 SW Brigadoon Ct, Beaverton OR 97005
 A. H. Peake
 ITT Gallium Arsenide Technology Center
 7670 Enon Dr, Roanoke VA 24019

ABSTRACT-A novel internal-node waveform probing technique has been demonstrated on a MMIC. The error of the measurement and its perturbation to circuit operation was estimated and verified to be less than 20%. Valuable insight was obtained from the variation of waveforms as a function of frequency, drive and location.

Internal-node waveform probing has been widely used to diagnose digital and analog integrated circuits under realistic operating conditions. With the availability of a 40 GHz sampling instrument and 26 GHz high-impedance probes, we developed a novel technique capable of internal-node probing of microwave waveforms [1]. In this paper, for the first time, we present the voltage and current waveforms measured at various locations within a MMIC power amplifier and without any layout modification or test structures. Based on the present set up and calibration procedure, the error of the measurement and its perturbation to circuit operation is estimated and verified to be less than 20%. The present approach offers a more practical alternative to other non-invasive probing techniques such as electro-optical probing.

The measurement set up (Fig. 1) and calibration procedure is similar to that described in [1], except the $500\ \Omega$ probe. The newly developed Cascade Microtech FPM probe does not require on-wafer grounding contact and has improved bandwidth, allowing up to the fifth harmonic of a 5 GHz input signal to be reliably measured. The non-invasive

nature of the present technique has been verified by comparing magnitudes and phases of the five output signal harmonics measured with and without probe contact. Figure 2 shows the variation in the output signal when the high-impedance probe is placed on the drain, the gate and the branch microstrip line of the MMIC unit cell. The results presented in the following were measured on a C-band, single-stage, 5 W, MMIC amplifier (Fig. 3). Each of the four MESFET unit cells comprises 20 gate fingers, each gate finger being $0.5\ \mu\text{m}$ long and $175\ \mu\text{m}$ wide.

Figure 4 shows the state-of-the-art power performance of the amplifier, measured at 5 GHz with a drain bias of 9 V and a gate bias of $-2\ \text{V}$. Similar performance was obtained from 4 to 6 GHz. Figure 5 illustrates the unit-cell drain and gate voltages at 5.375 GHz. These waveforms were measured on the unit-cell input and output lines, after all twenty fingers are interconnected and before any matching element is branched on. It can be seen that, under linear drive levels, the drain voltage lags the gate voltage by approximately 1 rad. Once the drive exceeds 26 dBm, which corresponds to approximately 1 dB gain compression, both waveforms are greatly distorted and their phase relationship becomes more ambiguous. Further, under heavy compression, the peak voltages can be twice the dc bias values. From the waveforms measured at different locations along each branch line, the total unit-cell drain and gate currents can be determined as shown in Fig. 6. Where it is possible to measure

the transmission line before and after it branches out, the sum of the branch currents was found to be within 20% of the total current. From the measured drain current and voltage waveforms, the dynamic load contour can be visualized as in Fig. 7. It can be seen that, with a relatively high load impedance, the drain voltage swings below the knee voltage, thereby achieving high power-added efficiency at the expense of saturated output power. However, such a high-impedance match also causes the drain voltage to swing higher which, together with a large gate-voltage swing, may exceed the threshold voltage for hot-electron-induced degradation [2]. Figure 8 shows that the peak drain-gate voltage measured with an input drive of 29 ± 1 dBm is higher than 15 V across the band. Such a peak voltage may cause gate-drain breakdown of the MESFET. To further illustrate the validity and utility of the present technique, Fig. 9 shows the magnitude of the drain and gate voltages measured on each unit cell. It can be seen that the variation in drain voltage is comparable to the measurement error, whereas significant variation in gate voltage exists between inner and outer unit cells.

In conclusion, a MMIC internal-node waveform probing technique has been developed and demonstrated. Valuable insight was obtained from the variation of waveforms as a function of frequency, drive and location. The peak voltage swing under different drive conditions was quantified. The variation of unit-cell characteristics within a MMIC was observed. Thus, the present technique can have broad impacts on MMIC design verification, reliability assessment, and process control.

REFERENCES

- [1] C. J. Wei, Y. A. Tkachenko and J. C. M. Hwang, "Non-invasive waveform probing for nonlinear network analysis," in *IEEE MTT-S Int'l Microwave Symp. Dig.*, May 1993, pp. 1347-1350.
- [2] Y. A. Tkachenko, Y. Lan, D. S. Whitefield, C. J. Wei, J. C. M. Hwang, T. D. Harris, R. D. Grober, D. M. Hwang, L. Aucoin and S. Shanfield, "Hot-electron-induced degradation of metal-semiconductor field-effect transistors," in *Technical Dig. IEEE GaAs IC Symp.*, Oct. 1994, pp. 259-262.

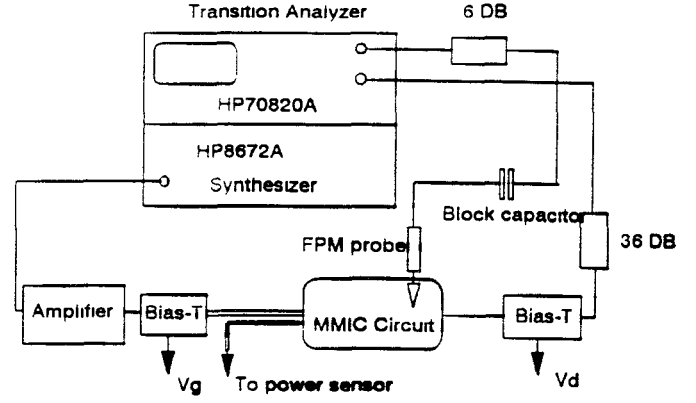
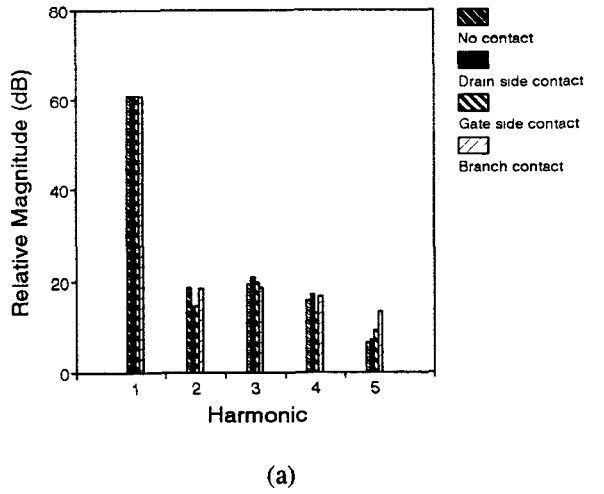


Figure 1. Waveform measurement setup



(a)

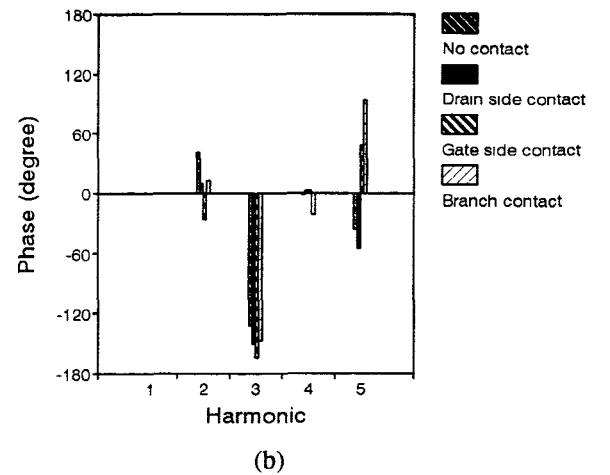


Figure 2. (a) magnitude and (b) phase variation in the unit cell output signal harmonics with and without probe contact.

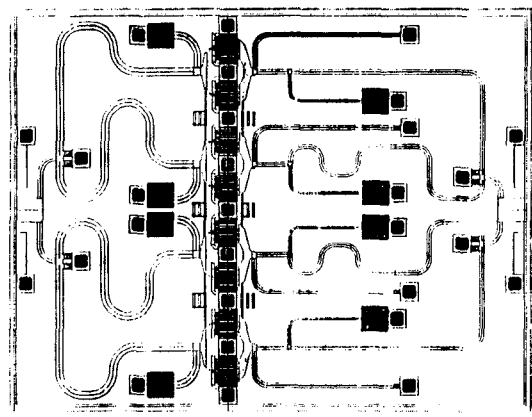


Figure 3. The schematic layout of an ITT C-band MMIC power.

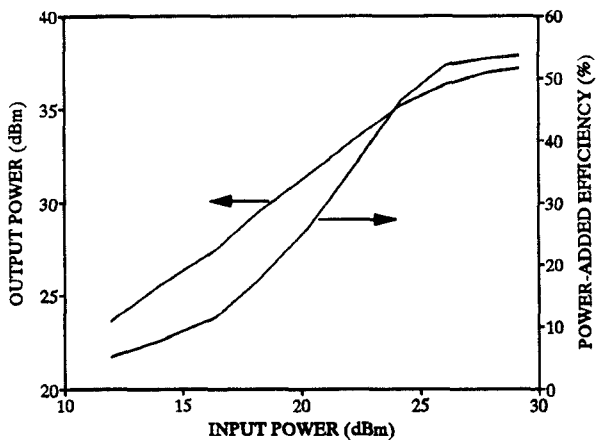
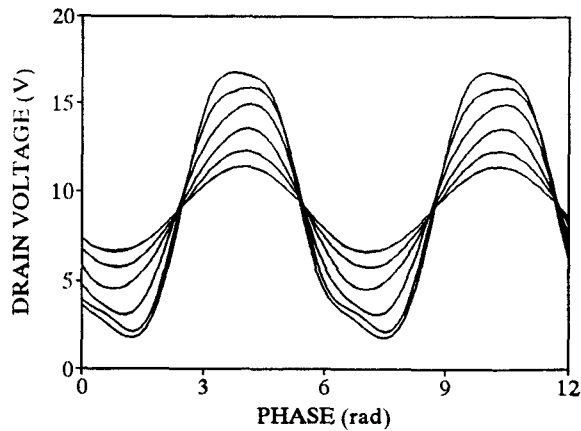
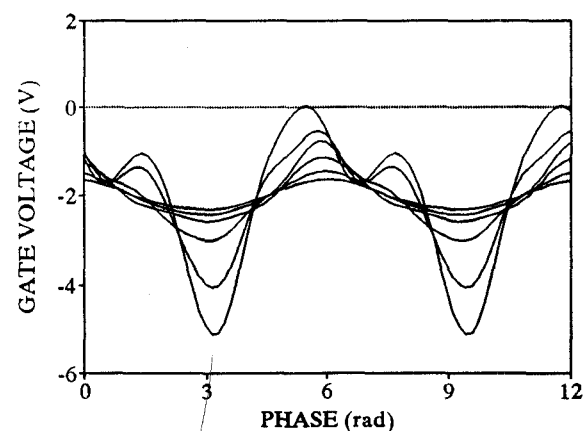


Figure 4. Power performance of the amplifier. $F = 5\text{GHz}$, $V_{ds} = 9\text{ V}$, $V_{gs} = -2\text{ V}$.

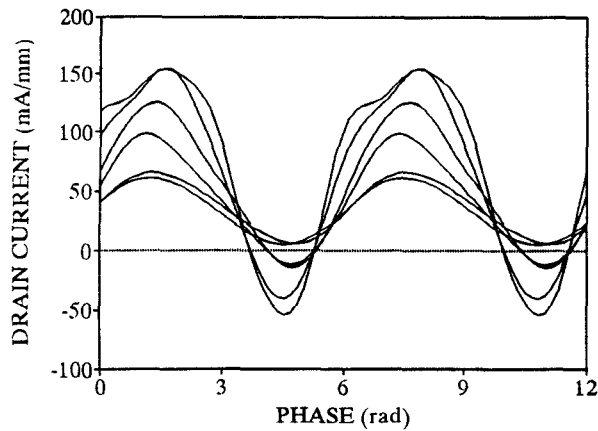


(a)

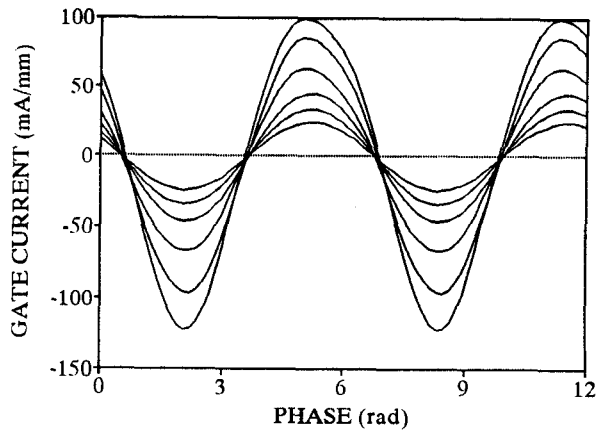


(b)

Figure 5. Unit cell (a) drain and (b) gate voltage waveforms. $F = 5.375\text{ GHz}$, $V_{ds} = 9\text{ V}$, $V_{gs} = -2\text{ V}$, $P_{in} = 13.6, 16.6, 19.6, 22.6, 25.6$ and 28.4 dBm



(a)



(b)

Figure 6. Unit cell (a) drain and (b) gate current waveforms. $F = 5.375\text{ GHz}$, $V_{ds} = 9\text{ V}$, $V_{gs} = -2\text{ V}$, $P_{in} = 13.6, 16.6, 19.6, 22.6, 25.6$ and 28.4 dBm .

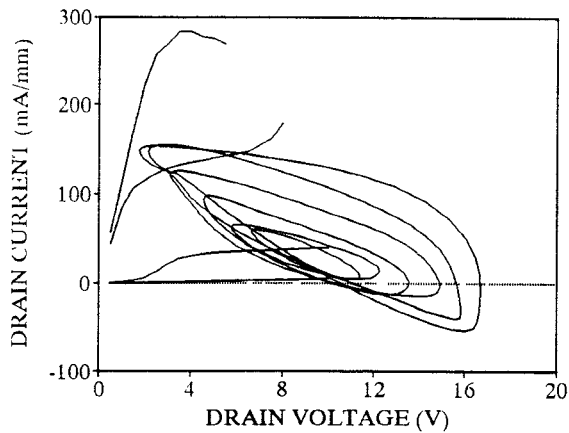


Figure 7. Unit cell dc and 5.375 GHz drain characteristics. At dc: $V_{gs} = 0, -1, -2$ and -3 V top down; at 5.375 GHz: $V_{ds} = 9$ V, $V_{gs} = -2$ V, $P_{in} = 13.6, 16.6, 19.6, 22.6, 25.6$ and 28.4 dBm.

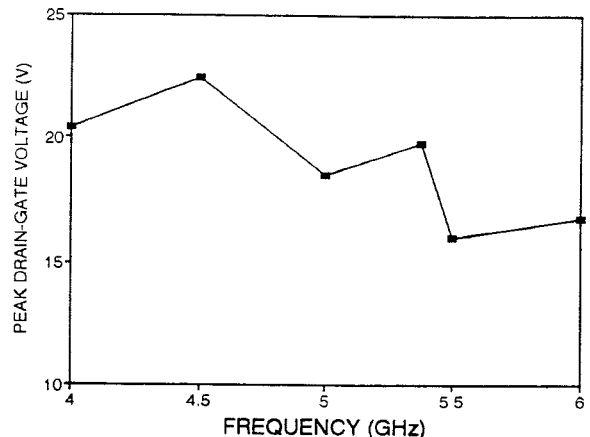


Figure 8. Peak drain-gate voltage measured across the band. $F = 5$ GHz, $V_{ds} = 9$ V, $V_{gs} = -2$ V, $P_{in} = 28 \pm 1$ dBm.

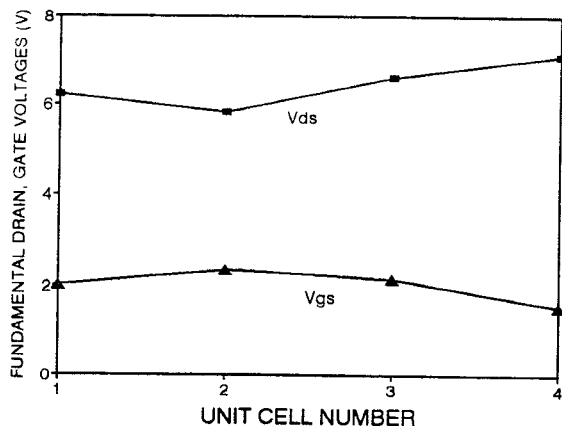


Figure 9. Variation in drain and gate voltage for different unit cells. $F = 5$ GHz, $V_{ds} = 9$ V, $V_{gs} = -2$ V.